

Solvent, Concentration and Temperature Effects in LiNi_{0.5}Mn_{1.5}O₄-Li₃PO₄ Coating Processes

Valeriu Mereacre,^{*[a]} Pirmin Stüble,^[a] and Joachim R. Binder^[a]

The spinel material LiNi_{0.5-x}Mn_{1.5+x}O₄ (LNMO) represents a very promising cathode candidate due to its high operating voltage and high specific capacity. Unfortunately, this material is suffering from capacity degradation and a low degree of cyclability at normal and elevated temperatures. Herein, using hydrogen peroxide (H₂O₂) as an activating reagent, an improvement of the spinel electrochemical properties is achieved by coating the spinel with Li₃PO₄. The coating method is simple,

has a low cost, it could be done in both organic or water solutions, and results in homogeneously coated particles. The structure and the electrochemical properties of the prepared cathodes were probed using XRD, SEM, EDS and electrochemical studies. It was established that the coating has a positive effect on the stability and performance of LNMO. As result, a long cycling stability and very good rate performance (~99% capacity retention over 300 cycles at 1 C) was achieved.

Introduction

Low battery cost and friendly impact on the environment are becoming increasingly important in the production of Li-ion batteries. Due to its high voltage and energy density, LiNi_{0.5-x}Mn_{1.5+x}O₄ (LNMO) is attracting considerable attention as a cathode material.^[1] Especially, its low cost (cobalt-free) makes it attractive for the lithium-ion battery industry. However, as with many other cathode materials,^[2,3] LNMO suffers from an unstable interfacial stability between the cathode and electrolyte. The application of diverse coating materials to LNMO can enhance its durability during the charging-discharging processes in batteries,^[4–8] as well as enhance its stability in the presence of moisture and oxygen environments.^[9] Recent research has also shown that Li₃PO₄ (LP) in LNMO-graphite full cells significantly reduces the deposition of transition metals on the anode side, resulting in considerable long-term stability.^[10]

Although LNMO is not very sensitive to moisture, a small change in the LNMO surface chemistry is possible. Due to its strong bonds and stable structure, the PO₄³⁻ ion could form stable metal phosphates on the LNMO surface. But such phosphates should also be Li ion conductive. A simple treatment with H₃PO₄ may result in products like MnPO₄ or NiPO₄, which are not conductive.^[11] Of course, in dependence on the conditions, the reaction with H₃PO₄ may also result in a coated LNMO with LP. However, the surface structure of the coated

active material can partially suffer because of the lost Li ions, which are consumed for the formation of LP.^[7] Therefore, it is important to introduce in the coating reaction not only H₃PO₄, but also enough Li ions to get an ion-conducting layer of LP.

The coating of cathode active materials with LP is largely documented in the literature.^[4–9,12,13] We propose in this work a novel approach using hydrogen peroxide (H₂O₂) as an activating reagent. The presented coating method is successfully used in our group for coating LNMO and NCM cathode active materials.^[14–18] There was no doubt that this technique will also work for LP in laboratory conditions. However, to use this method on an industrial level, optimization is needed. First, this method is very risky if the reaction is done in concentrated hydrogen peroxide.^[14–17] Second, the decomposition of hydrogen peroxide in the presence of manganese-containing oxides^[19–21] is a strongly exothermic reaction and if the reaction medium is getting hot, the decomposition rate of the H₂O₂ could be uncontrollable. We have succeeded to optimize this reaction making the coating process in water and ethanol solutions. The result was almost the same as when using a concentrated H₂O₂ solution. The only drawback is that the reaction takes longer: in H₂O₂ – two hours, and in aqueous or alcoholic solutions – more than 24 hours. In addition to minimizing the risk of an accident, using the optimized reactions, one can also reduce the probability of pre-damage of the particles with H₂O₂ before the beginning of the coating process. As reported by us earlier, a simple treatment of LNMO only with concentrated (30%) H₂O₂ resulted in a partially damaged surface of the particles.^[16] Although big damages on the surface were not observed in the present work after the coating processes, such a property of H₂O₂ must be taken into account. In this study, three novel synthetic approaches were elaborated for the coating of cathode materials with lithium phosphate. Scanning electron microscopy (SEM) together with energy dispersive X-ray (EDS) and Powder X-ray diffraction (PXRD), combined with electrochemical property measurements were used to identify the differences between the three techniques.

[a] V. Mereacre, P. Stüble, J. R. Binder

Institute for Applied Materials, Energy Storage Systems, Karlsruhe Institute of Technology, Hermann-von-Helmholtz-Platz 1, D-76344 Eggenstein-Leopoldshafen, Germany

E-mail: valeriu.mereacre@kit.edu

 Supporting information for this article is available on the WWW under <https://doi.org/10.1002/batt.202400666>

 © 2024 The Author(s). *Batteries & Supercaps* published by Wiley-VCH GmbH. This is an open access article under the terms of the Creative Commons Attribution Non-Commercial NoDerivs License, which permits use and distribution in any medium, provided the original work is properly cited, the use is non-commercial and no modifications or adaptations are made.

Experimental

Materials Preparation

The precursor for LNMO was obtained by a co-precipitation technique described elsewhere.^[14–16] In a typical synthesis route, 0.185 mol of analytical reagent grade LiCH₃COO·2H₂O, 0.090 mol Ni(CH₃COO)₂·4H₂O, and 0.270 mol Mn(CH₃COO)₂·4H₂O (all supplied by Alpha Aesar, Kandel, Germany) were dissolved in 300 mL of water. The obtained solution was transferred into a 1 L continuously stirred tank reactor. Separately, 0.451 mol of H₂C₂O₄·2H₂O were dissolved in 450 ml of water. Under a temperature of 50°C and constant stirring (400 rpm) of the Li–Ni–Mn solution, 30 g of solid PEG6000 was added. After 10 minutes, when PEG6000 dissolved completely, the oxalic acid aqueous solution was started to be pumped (10 ml/min) into the continuously stirred tank reactor. After the oxalic acid solution was completely pumped, the reaction mixture was stirred for an additional 20 minutes. Then, the obtained suspension was dried at 90°C to obtain a green viscous precursor (~85 g). The resultant precursor was calcined in air at 450°C for 4 h and then at 900°C for 24 h, and cooled down to room temperature with the heating and cooling rate of 4°C/min to obtain the LiMn_{1.5}Ni_{0.5}O₄, which is labelled as LNMO. Brunauer–Emmett–Teller (BET) surface area is 0.35 m²g⁻¹. The reference compounds, LNMO-550 and LNMO-800, were obtained by calcining pristine LNMO in the air at 550 and 800°C, respectively, using the following program: 250°C for 2 h and then heated at the indicated temperature for 5 h with the heating rate of 4°C/min, and cooled down to room temperature with the cooling rate of 2°C/min.

The LP coating solution was prepared as follows: 0.27 g reagent-grade lithium acetate (LiOOCCH₃·2H₂O) (Alfa Aesar, Kandel, Germany) and 0.10 g phosphoric acid (85%), (Aldrich, Steinheim, Germany) were dissolved in a mixture of 30 ml H₂O₂ (30%) (Aldrich, Steinheim, Germany) and 0.5 ml concentrated nitric acid (HNO₃) (Fischer Scientific, Loughborough, UK). The obtained mixture was stirred until a clear solution was obtained.

Material Coating

Hydrogen peroxide (H₂O₂) method: In a round bottom flask (1000 ml) with 1.0 g LNMO 20 ml H₂O₂ (30%) were added. Under stirring, after ~30 seconds, 1.8 ml LP coating solution slowly (~2 drops/s) was added. During the next 90 minutes the reaction was relatively silent, but after this time, the reaction started to be very violent forming a white fog. The violent reaction takes place in less than 20 minutes. After an additional 5 minutes of stirring, when the decomposition of H₂O₂ has stopped, the reaction mixture was decanted, the obtained powder was washed with 30 ml water, centrifuged, and dried for one hour at 80°C. The obtained dry powder (LNMO-LP-80H) was divided into two portions and calcined in air at 550 and 800°C using the following program: 250°C for 2 h and then heated at a particular T °C for 5 h with the heating rate of 4°C/min, and cooled down to room temperature with the cooling rate of 2°C/min. The quantity of the LP expected to be coated on the surface of LNMO particles is around 0.5 wt% LP (Table S1). The obtained samples were labelled as LNMO-LP-550H and LNMO-LP-800H, respectively.

A similar reaction was made with 18.2 ml LP coating solution, resulting in LNMO particles coated with approximately 5 wt% LP. The obtained sample was divided into two portions and calcined in air at T=550 and 800°C, and labelled as LNMO-LP-550H(5%) and LNMO-LP-800H(5%), respectively.

Ethanol (C₂H₅OH) method: In a round bottom flask (500 ml) with 1.0 g LNMO 30 ml C₂H₅OH (water-free) were added. Under stirring,

after 15 minutes, 1.8 ml LP coating solution diluted with 10 ml H₂O₂ (30%) slowly was added. The reaction was very slow and even after 25 hours (under permanent stirring) slow elimination of gases was observed. Although the decomposition of H₂O₂ has not stopped, nevertheless the reaction mixture (after 25 hours) was decanted, and the obtained powder (coated with approximately 0.5 wt% LP) once washed with 30 ml ethanol, centrifuged, and dried for one hour at 80°C. The obtained dry powder (LNMO-LP-80E) was divided into two portions and calcined using the same programs as above (550°C and 800°C). The obtained samples were labelled as LNMO-LP-550E and LNMO-LP-800E, respectively.

A similar reaction was made with 18.2 ml LP coating solution (without dilution with 10 ml H₂O₂), resulting in LNMO particles coated with approximately 5 wt% LP. The obtained sample was divided into two portions and calcined in air at T=550 and 800°C, and labelled as LNMO-LP-550E(5%) and LNMO-LP-800E(5%), respectively. This reaction was also very slow and was also stopped after 25 hours.

Water (H₂O) method: similar to C₂H₅OH method, but in place of ethanol water was used. The obtained powder (coated with approximately 0.5 wt% LP) after 25 hours was one time washed with 30 ml H₂O, centrifuged, and dried for one hour at 80°C. The obtained dry powder (LNMO-LP-80W) was divided into two portions and calcined using the same programs as above (550°C and 800°C). The obtained samples were labelled as LNMO-LP-550W and LNMO-LP-800W, respectively.

A similar reaction was made with 18.2 ml LP coating solution, resulting in LNMO particles coated with approximately 5 wt% LP. The obtained sample was divided into two portions and calcined in air at T=550 and 800°C, and labelled as LNMO-LP-550W(5%) and LNMO-LP-800W(5%), respectively. This reaction was also very slow and, as in the case of the 0.5% sample, was also stopped after 25 hours.

Powder X-ray Diffraction and Scanning Electron Microscope

Powder X-ray diffraction (PXRD) patterns were recorded with a Bruker D2Phaser Diffractometer in Bragg-Bretano configuration using Cu-K_α radiation and a LynxEye_XE_T detector. The measurements were carried out in the range of 10° < 2θ < 80°, with a step width of 0.02° and step time of 1 s per step. Powder samples were loaded onto a low-background Si sample holder. Crystal structures and phase compositions were refined using the Rietveld method^[22] with the TOPAS 6 software. A correction term was used to compensate for the sample displacement resulting from the specimen preparation. A uniform isotropic displacement parameter B = 0.5 was used for all atomic positions and temperatures. Profile broadenings were modelled using common parameters for crystal size and strain broadening, as described in previous work.^[23]

A scanning electron microscope SEM (Zeiss Supra 55, Oberkochen, Germany) was used to elucidate the morphology of the coated samples. Before measurement the samples were prepared by mounting the powder on adhesive carbon tape. The energy dispersive X-ray spectroscopy (EDS) was carried out using EDS Detector Apollo 40 SSD, EDAX Inc., USA with an acceleration voltage of 7 kV. After the sample was coated on aluminium foil and dried, a small piece of it was cut and the broad-ion beam slope cutting (BIBSC) method was employed (using Ion Beam Milling System Leica EM TIC 3X) to produce cross-sections with smooth surfaces.

Electrochemical Measurements

Electrochemical measurements were carried out via galvanostatic charge/discharge cycling using 2032 coin cells with lithium metal as the anode on an BT2000 battery cycler (Arbin Instruments, College Station, Texas, USA). During electrode preparation, the slurry was a mixture of 80 wt% active material, 10 wt% Super-S carbon black (Timcal, MTI Corporation, Richmond, CA, USA), and 10 wt% PVDF (Polyvinylidene fluoride) with NMP (1-Methyl-2-pyrrolidinone) as solvent. Electrodes were prepared by coating the slurry on an Al foil with a 200 μm notch bar spreader and dried in air at 80°C for 20 minutes, then at 100°C for 16 hours in a vacuum. Usual cathode loadings were in the range of 4.0–5.0 mg cm^{-2} ; an electrode diameter of 12 mm was used. Before use the cathode disks were pressed in a hydraulic press to 5 kN and dried additionally for 60 minutes in a vacuum oven at 110°C. The electrolyte (200 μL for every coin cell) was 1.0 M LiPF₆ solution in 1:1 v/v ethylene carbonate:diethyl carbonate (EC:DMC). As anode a lithium metal foil (diameter 12 mm) was used. As separators were used one layer of Celgard 2325 (Celgard, Sélestat, France) on the lithium side, one layer on the positive electrode, and one GFC microfiber separator in the middle. We have made four different cells: with a GFC microfiber separator, with a Celgard separator, with GFC microfiber separator and Celgard separator and, as in the present paper, with Celgard/GFC/Celgard. The final combination was demonstrated to be the most efficacious in preventing dendrite growth through the separator and was utilized for all cells. Cells were assembled in a dry Ar-filled glove box. Cycling was performed at a temperature of 23°C. A voltage window of 3.5–4.9 V vs. Li⁺/Li was applied.

Results and Discussion

Coating Material

To achieve a good mixing of different components during a synthesis, very often the sol-gel method is used.^[24–26] This method seems to be the most suitable when the target is to obtain very good mixed elements at molecular level. Especially, it is worthy to use this method when the goal is to synthesize efficient and stable coated battery materials.^[27,28] LP is widely used for the coating of different cathode active materials.^[29–34] Although its structure could facilitate the Li ion diffusion, which would result in a good ionic conductivity at room temperature, this material as a coating will not improve the electronic conductivity of the cathode materials. In the form of a thin coating layer, however, it should not affect dramatically the electrode/electrolyte interface communication. Hence, in this

study two concentrations of LP were used: 0.5 wt% LP coated LNMO for electrochemical studies and 5 wt% LP coated LNMO for the structural studies of the obtained coating. For the NMC layered oxides, especially Ni-rich, which suffer from the presence of Li₂O/LiOH/Li₂CO₃ residues on the cathode surface, an efficient method for the coating might be the treatment with phosphoric acid. This will result in its reaction with Li₂O/LiOH/Li₂CO₃ residues and formation on the surface of a LP coating.^[29] A collateral reaction, however, is not excluded: the phosphoric acid can partially react with active material, resulting in Mn/Ni/Co phosphates. This reaction can take place on the surface of the NMC layered oxides, but it is also possible for more “rigid” oxides, like, for example, LNMO spinel. However, due to the inactive manganese or nickel phosphate, which will form on the spinel surface, the obtained coated active cathode material may show a low performance.^[11] Therefore, in this work as coating material is used a mixture of phosphoric acid and a lithium salt.

Given the specific surface area of 0.35 m^2/g for the pristine LNMO material and a density of 2.45 g/cm^3 for Li₃PO₄, the 0.5 wt% and 5.0 wt% LP layers are expected to have a thickness of ~5.8 nm and ~58 nm, respectively, when a homogeneous coating is assumed.

Scanning Electron Microscopy (SEM)

SEM images of the samples discussed in this work are shown in Figures 1–3. Figure 1 shows the pristine, uncoated LNMO, treated at 80, 550 and 800°C. The bare sample was exposed to these temperatures in order to check how additional temperature treatment influence the surface of the particles. As a result, additional temperature treatment caused no or minor changes; the obtained SEM images show smooth and clean particles with similar surface morphology.

In Figure 2(a–c) are presented LNMO particles coated with 0.5 wt% LP using three different methods and dried at 80°C. The surface of the coated LNMO becomes rougher and the obtained result cannot point to just a simple erosion of the LNMO surface by H₂O₂. It points to a coherent surface layer. No damages are observed on the surface of the coated particles, as was the case when LNMO reacts with pure H₂O₂^[15]; it can be assumed, that during the decomposition of H₂O₂, lithium and phosphate compounds precipitate on the LNMO surface and protect it from further reaction with H₂O₂.

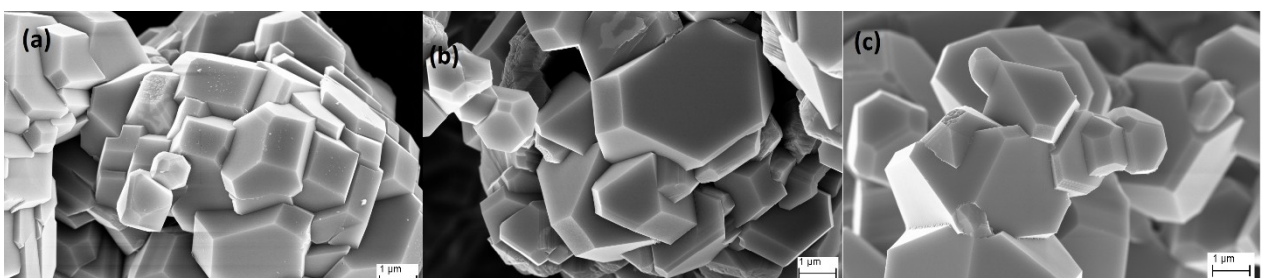


Figure 1. SEM diagrams of pristine LNMO dried at 80 °C (a), calcined at 550 °C (b) and calcined at 800 °C (c).

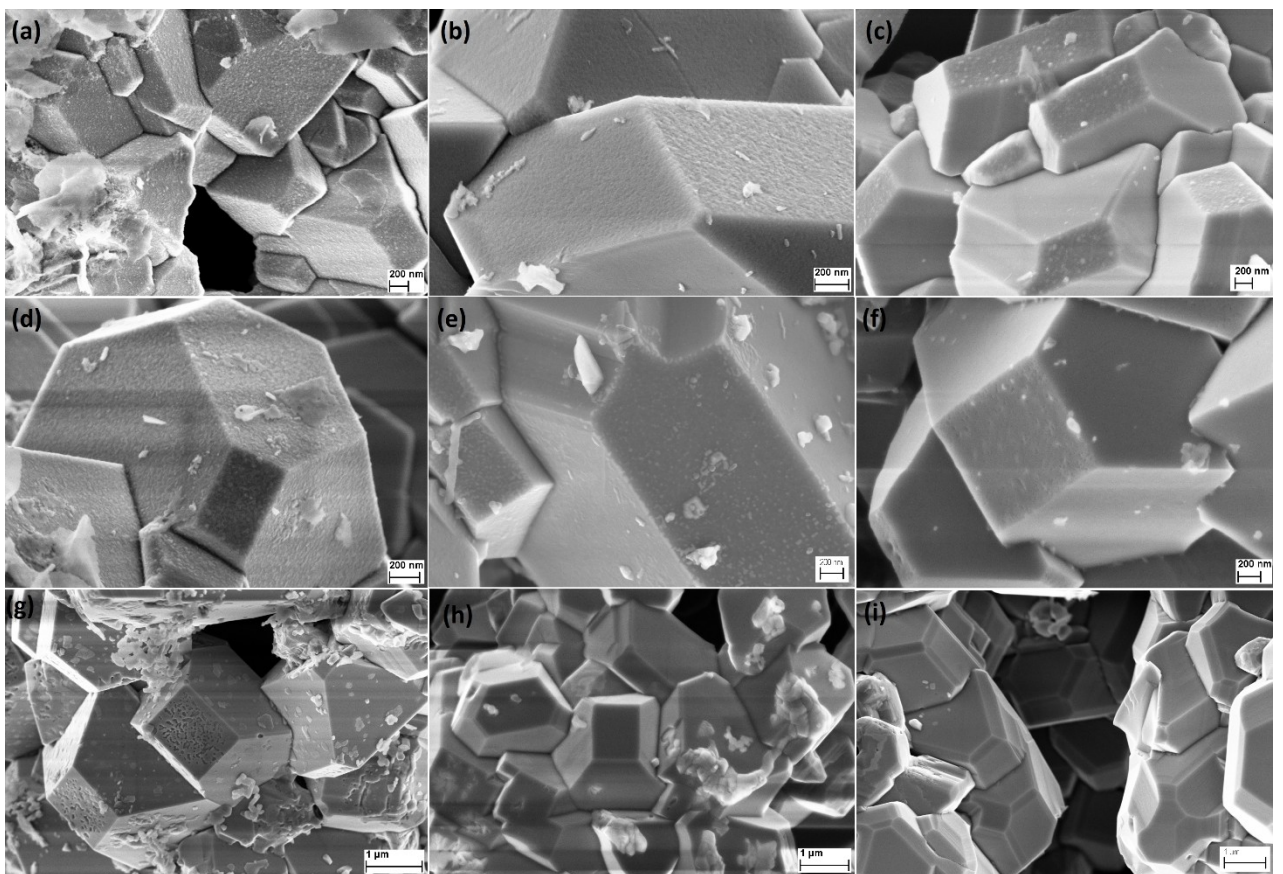


Figure 2. SEM diagrams of samples coated with 0.5 wt% LP: LNMO-LP-80H (a), LNMO-LP-80E (b) and LNMO-LP-80W (c) dried at 80 °C, LNMO-LP-550H (d), LNMO-LP-550E (e) and LNMO-LP-550W (f) calcined at 550 °C and LNMO-LP-800H (g), LNMO-LP-800E (h) and LNMO-LP-800W (i) calcined at 800 °C.

The major difference between LNMO-LP-80H, LNMO-LP-80E, and LNMO-LP-80W compounds is the presence of an abundant quantity of crystalline flakes in case of the sample obtained in hydrogen peroxide and fewer flakes in the case of sample coated in water. The crystalline flakes represent well-dispersed nanoplates of a porous structure without much stacking. For the sample coated in ethanol, the impurity is also present, but in minor quantities. The crystallinity of the flakes was determined by XRD study of the 5 wt% LP coated sample in H₂O₂ directly after drying at 80 °C without calcination (Figure S1). The diffraction pattern shows several reflections, which are not possible to assign to any known compound. It is assumed that these reflections correspond to compounds that crystallize only in the presence of LNMO. The thermal treatment at 550 °C (Figure 2d-f) did not bring great changes in the morphology of the coating. At 800 °C (Figure 2g-i), however, there are some differences, which are worth to be discussed. As was mentioned earlier,^[15] if the LNMO reacts with pure hydrogen peroxide (30%), the decomposition reaction partially damages the surface of the truncated octahedral crystals; especially the {100} facets are damaged. As can be seen in Figure 2g-i, the truncated surfaces of the LNMO-LP-800E and LNMO-LP-800W crystals are smooth and intact. On the other hand, the coating on the same surfaces of the LNMO-LP-800H crystals has an eroded and incomplete structure. The exact

reason for such a behavior is not known, but it is assumed that such a phenomenon is owing to the higher reactivity of {100} facets, compared to the {111} ones. It is assumed that such effects are not seen for LNMO-LP-800E and LNMO-LP-800W, because the coating reactions for these two samples were done in ethanol and water, resulting in diluted media and respectively less hydrogen peroxide. A second aspect, that has to be taken into account is that at 800 °C there are significant changes in the composition of LNMO materials. Compared to the samples treated at 80 °C and 550 °C, at 800 °C pronounced solid-state reactions occur, which affect not only the surface, but the bulk material as well. The proportion of secondary phases increases to around 20%, while the LNMO phase is depleted in Li and Ni.^[1] Although these processes are largely reversible in principle, here, the composition of the spinel phase can be changed by the coating material.

To better understand these processes and to detect the morphology of the coated product and of the co-crystallized impurities by means of PXRD and SEM, the LNMO material was coated with an increased LP coating amount (~5%) (Figure 3). The obtained powders were also calcined at 550 and 800 °C (Figures 3d-i). The SEM images of the LNMO material coated with 5 wt% LP and calcined at different temperatures clearly show the presence of a thick layer of the coating material on the surface of the active substance LiMn_{1.5}Ni_{0.5}O₄. Some SEM

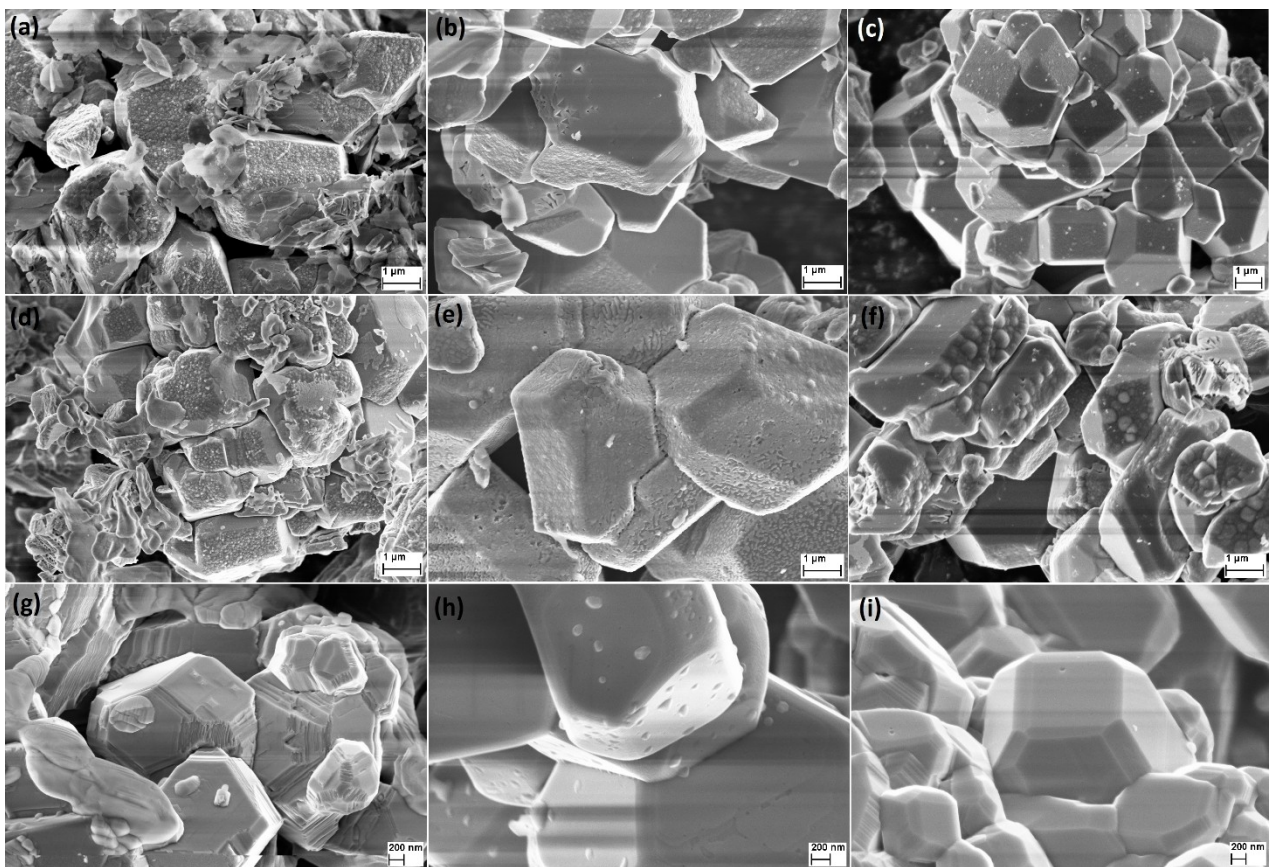


Figure 3. SEM diagrams of samples coated with 5 wt % LP: LNMO-LP-80H(5%) (a), LNMO-LP-80E(5%) (b) and LNMO-LP-80W(5%) (c) dried at 80 °C, LNMO-LP-550H(5%) (d), LNMO-LP-550E(5%) (e) and LNMO-LP-550W(5%) (f) calcined at 550 °C, and LNMO-LP-800H(5%) (g), LNMO-LP-800E(5%) (h) and LNMO-LP-800W(5%) (i) calcined at 800 °C.

and energy dispersive X-ray (EDS) examinations of the particle's surface were carried out and confirmed the presence of P in the coated film. LNMO-LP-800W and LNMO-LP-550E(5%) were selected as representative examples, Figures S2 and S3, respectively. The EDS results reflect the quantity of P in dependence on the concentration of the coating solution and the examined part of the particles and confirm the presence of a P-rich or P-poor coating. Cross-sectional SEM image and EDS line scan for P-elemental distribution for the sample LNMO-LP-550E(5%) (Figures S4 and S5) also confirm the presence of a P-rich coating. As in the case of samples coated with 0.5 wt % coating material, the sample obtained in hydrogen peroxide and coated with 5 wt % LP, in comparison with the other two, shows the presence of a plentiful quantity of crystalline flakes. One of the reasons could be the fact that the reaction in H₂O₂ takes place too fast and some amount of lithium and phosphate ions do not succeed to coat, but interact with each other out of the LNMO surface. On the other hand, the SEM images of the other two samples (LNMO-LP-550E(5%) and LNMO-LP-550W(5%)) show that the coating process in ethanol or water results in fewer secondary products. Another point worth discussing is the morphology of the coating at 800 °C. In all samples, the edges of the LNMO particles are affected. For the sample LNMO-LP-800H(5%) this leads to an assembly of uniformly overlapping nano sheet-like structures on the surface of LNMO.

For LNMO-LP-800E(5%) the edges and the tips are rounded and for LNMO-LP-800W(5%) the tips remain practically unchanged, but the edges look like they would have been carved. The changes in the lattice parameters of LNMO (see below) indicate pronounced reactions of the spinel phase with the coating material.

Comparable reactions are not observed at 550 °C. At this temperature, the formation of secondary phases is not yet favored and LNMO is thermodynamically stable.^[1] From Figure 3d-f, it can be concluded that the surface is totally covered by the coating, but the coating did not yet influence the LNMO morphology. However, minor differences in the coating surface can likewise be observed. LNMO-LP-550H(5%) appears to have additional secondary phase particles. LNMO-LP-550E(5%) and LNMO-LP-550W(5%) show more homogeneous coating layers overall.

The reasons for the variation of the morphologies at each temperature are most likely different reaction conditions (H₂O₂, ethanol and, water). Nevertheless, the phase analysis clearly shows that H₂O₂, ethanol, and water, yield similar coating products and bulk material properties for each temperature treatment, as shown next.

Phase Analysis

The PXRD patterns of pristine LNMO and LNMO calcined at 550 and 800 °C are shown in Figure 4. The corresponding phase fractions and lattice parameters are outlined in Table 1. A disordered structure model (space group $Fd\bar{3}m$) and ideal composition $\text{LiNi}_{0.5}\text{Mn}_{1.5}\text{O}_4$ were used for the refinement of the

LNMO phase. The exact transition metal content of LNMO cannot be determined by means of PXRD because of the similar scattering length of Ni and Mn. Based on the analysis of the voltage profiles shown in Figure S7, the composition of the spinel phase is roughly $\text{LiNi}_{0.44}\text{Mn}_{1.46}\text{O}_4$ (LNMO-44) to $\text{LiNi}_{0.45}\text{Mn}_{1.45}\text{O}_4$ (LNMO-45),^[1] which is very common for disordered LNMO materials. All three diffraction patterns shown in Figure 4 also reveal typical reflections of a cubic rocksalt-type secondary phase, which was refined using a $Fm\bar{3}m$ model with the composition $\text{Li}_{0.33}\text{Ni}_{0.44}\text{Mn}_{0.22}\text{O}$ ($a \approx 414$ pm). In addition, a small amount of a Li and Ni-rich secondary phase with a layered structure (N-layered) is present in the pristine sample. This secondary phase was refined as $\text{Li}_{0.4}\text{Ni}_{0.6}\text{O}$ with $\alpha\text{-NaFeO}_2$ structure-type ($R\bar{3}mH$, $a \approx 293.4$ and $c \approx 1430.8$ pm) with a structure model from Ref. .^[35] As discussed in a previous work, the presence of such layered side phases becomes obvious from a shoulder of the LNMO 111 at $2\theta \approx 18.5^\circ$. From the good agreement with high temperature PXRD experiments^[1] and the electrochemical data shown below, it is evident that with the thermal treatment at 550 and 800 °C, the overall content of the LNMO phase increases and the overall side phases decreases. This provides a conclusive explanation for the slightly higher discharge capacities of the samples that underwent an additional thermal treatment at 550 and 800 °C, respectively (vide infra).

The diffraction patterns and corresponding refinements for the coated samples using the H_2O_2 method are shown in Figure 5. The corresponding figures for the ethanol and water methods are shown in Figures 6 and 7, respectively.

With one exception (see below), the Ni-rich layered side phase found in the pristine sample could likewise be confirmed

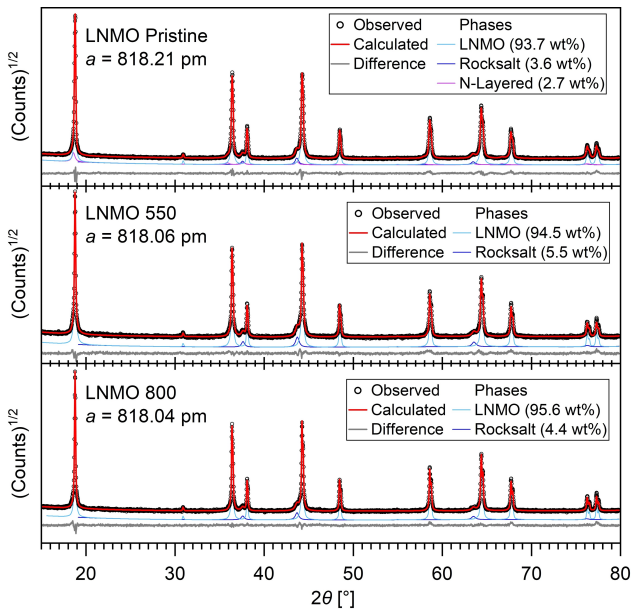


Figure 4. Rietveld refinements of pristine LNMO and LNMO calcined at 550 and 800 °C. The contributions of the individual crystalline phases are shown and set off vertically for the sake of clarity.

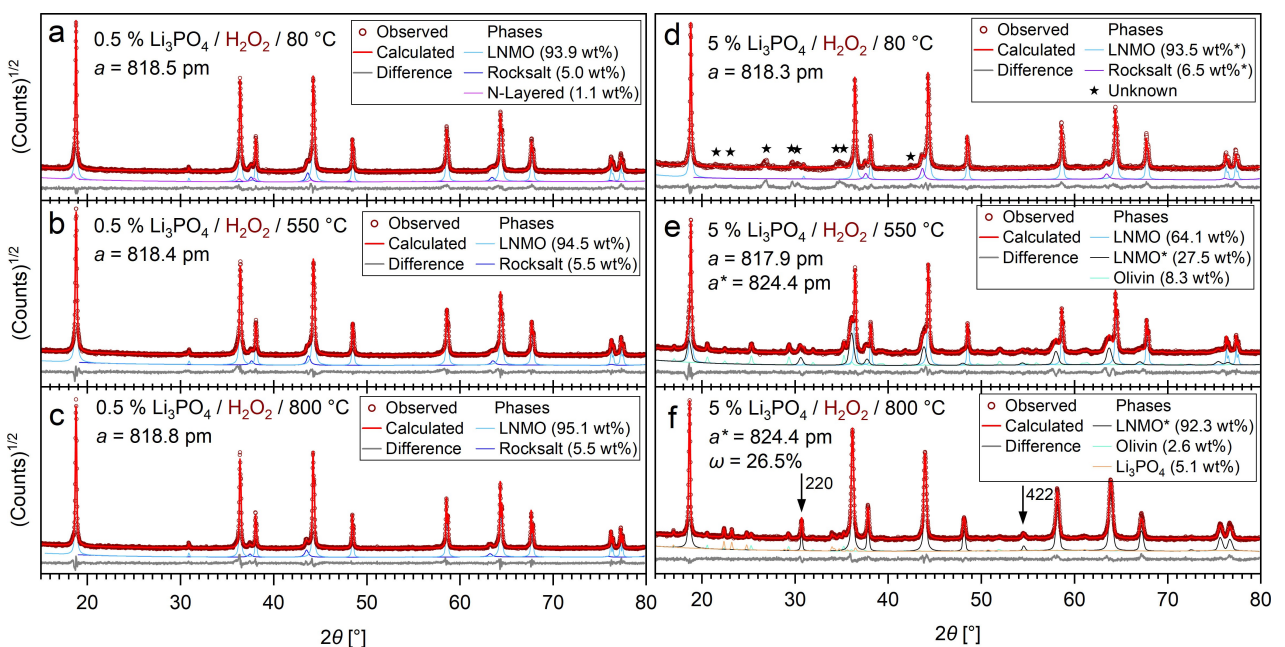


Figure 5. Rietveld refinements of the different LNMO materials coated with the hydrogen peroxide method with 0.5 and 5.0 wt % LP after thermal treatments at 80, 550 and 800 °C. The contributions of the individual crystalline phases are shown and set off vertically for the sake of clarity. Reflections that could not be assigned to any known compound are marked with black stars. Increased intensities of the 220 and 422 spinel phase reflections are marked by black arrows and indicate the occupation 26.5% of the Li-site with transition metal ions. The corresponding composition of the LNMO* phase is estimated to be around $\text{Li}_{0.73}\text{Ni}_{0.5}\text{Mn}_{1.77}\text{O}_4$.

Table 1. Detailed results of the Rietveld refinements (e.s.d.). LNMO* is a spinel phase with ~25% occupation of transition metal ions at the Li site (Wyckoff position 8b). *Sample LNMO-LP-80H(5%) contains at least one unindexed crystalline phase which could not be refined and which probably accounts for 2–5 wt %.

Sample	T, °C	Rietveld-Refinement									
		R _{wp}	LNMO (<i>Fd-3 m</i>)	a [pm]	x [wt%]	a [pm]	x [wt%]	Rocksalt (<i>Fm-3 m</i>)	a [pm]	x [wt%]	Ni-rich layered (<i>R-3mH</i>)
LNMO pristine		6.6	818.214(8)	93.7(2)	414.61(7)	3.6(2)	293.4(2)	1430.8(1.7)			2.7(2)
LNMO-550		7.1	818.059(8)	94.5(2)	414.15(5)	5.5(2)	—	—			—
LNMO-800		6.8	818.044(6)	95.6(1)	414.34(6)	4.4(1)	—	—			—
LNMO-LP-80H	80 °C	H ₂ O ₂	7.0	818.511(8)	93.9(2)	414.70(6)	5.0(2)	290.2(2)	1436.4(1.2)	1.1(2)	
LNMO-LP-80W	80 °C	H ₂ O	7.2	818.523(7)	93.2(2)	415.05(6)	5.4(2)	289.7(2)	1437.3(9)	1.4(2)	
LNMO-LP-80E	80 °C	EtOH	8.3	818.372(10)	93.6(2)	414.82(7)	4.7(2)	290.2(2)	1434.5(9)	1.7(2)	
LNMO-LP-550H	550 °C	H ₂ O ₂	8.2	818.396(8)	94.5(1)	414.16(7)	5.5(1)	—	—		—
LNMO-LP-550W	550 °C	H ₂ O	9.2	818.127(8)	94.2(2)	414.19(7)	5.8(2)	—	—		—
LNMO-LP-550E	550 °C	EtOH	9.4	817.948(8)	94.7(2)	414.38(7)	5.3(2)	—	—		—
LNMO-LP-800H	800 °C	H ₂ O ₂	8.8	818.835(6)	95.1(2)	415.95(7)	4.9(2)	—	—		—
LNMO-LP-800W	800 °C	H ₂ O	8.1	818.321(6)	94.9(2)	415.60(6)	5.1(2)	—	—		—
LNMO-LP-800E	800 °C	EtOH	7.5	818.151(5)	94.9(2)	415.54(6)	5.1(2)	—	—		—
LNMO-LP-80H(5%)	80 °C	H ₂ O ₂	10.0	818.318(12)	93.5(3)*	414.84(8)	6.5(2)*	—	—		—
LNMO-LP-80W(5%)	80 °C	H ₂ O	6.5	818.308(6)	93.4(2)	414.87(5)	5.1(2)	289.1(2)	1438.2(1.3)	0.9(1)	
LNMO-LP-80E(5%)	80 °C	EtOH	7.3	818.679(8)	92.8(2)	415.17(6)	5.5(2)	290.5(2)	1438(9)	1.7(2)	
LNMO (<i>Fd-3 m</i>)											
a [pm] x [wt%] a [pm] b [pm] c [pm] x [wt%] a* [pm] b [pm] c [pm] x [wt%]											
LNMO-LP-550H(5%)	550 °C	H ₂ O ₂	8.3	817.925(10)	64.1(3)	1043.1(3)	609.1(2)	474.4(2)	8.3(2)	824.41(4)	27.6(3)
LNMO-LP-550W(5%)	550 °C	H ₂ O	9.6	817.821(10)	74.8(4)	1043.8(4)	610.4(2)	474.8(3)	6.7(2)	825.12(8)	18.3(4)
LNMO-LP-550E(5%)	550 °C	EtOH	7.9	817.889(8)	76.4(3)	1043.9(3)	610.6(2)	474.8(2)	7.0(2)	825.74(6)	16.6(3)
LNMO* (<i>Fd-3 m</i>)											
a [pm] x [wt%] a [pm] b [pm] c [pm] x [wt%] a* [pm] b [pm] c [pm] x [wt%]											
LNMO-LP-80H(5%)	800 °C	H ₂ O ₂	6.3	824.441(10)	92.3(2)	1043.5(4)	610.3(2)	475.0(2)	2.6(1)	492.97(13)	611.58(18)
LNMO-LP-800W(5%)	800 °C	H ₂ O	5.6	824.583(7)	92.3(2)	1045.8(6)	610.4(3)	474.8(3)	1.1(1)	492.89(7)	612.04(9)
LNMO-LP-800E(5%)	800 °C	EtOH	5.6	824.747(7)	92.2(2)	1042.1(6)	608.8(3)	474.5(3)	1.2(1)	491.45(7)	612.35(9)
Olivin-Phase (<i>Pnma</i> ; ~LiMnPO ₄)											
a [pm] x [wt%] a [pm] b [pm] c [pm] x [wt%] a* [pm] b [pm] c [pm] x [wt%]											
LNMO-LP-80H(5%)	800 °C	H ₂ O ₂	6.3	824.441(10)	92.3(2)	1043.5(4)	610.3(2)	475.0(2)	2.6(1)	492.97(13)	611.58(18)
LNMO-LP-800W(5%)	800 °C	H ₂ O	5.6	824.583(7)	92.3(2)	1045.8(6)	610.4(3)	474.8(3)	1.1(1)	492.89(7)	612.04(9)
LNMO-LP-800E(5%)	800 °C	EtOH	5.6	824.747(7)	92.2(2)	1042.1(6)	608.8(3)	474.5(3)	1.2(1)	491.45(7)	612.35(9)
Li _{1-x} PO ₄ (<i>Pcmn</i>)											
a [pm] x [wt%] a [pm] b [pm] c [pm] x [wt%]											
LNMO-LP-80H(5%)	800 °C	H ₂ O ₂	6.3	824.441(10)	92.3(2)	1043.5(4)	610.3(2)	475.0(2)	2.6(1)	492.97(13)	611.58(18)
LNMO-LP-800W(5%)	800 °C	H ₂ O	5.6	824.583(7)	92.3(2)	1045.8(6)	610.4(3)	474.8(3)	1.1(1)	492.89(7)	612.04(9)
LNMO-LP-800E(5%)	800 °C	EtOH	5.6	824.747(7)	92.2(2)	1042.1(6)	608.8(3)	474.5(3)	1.2(1)	491.45(7)	612.35(9)

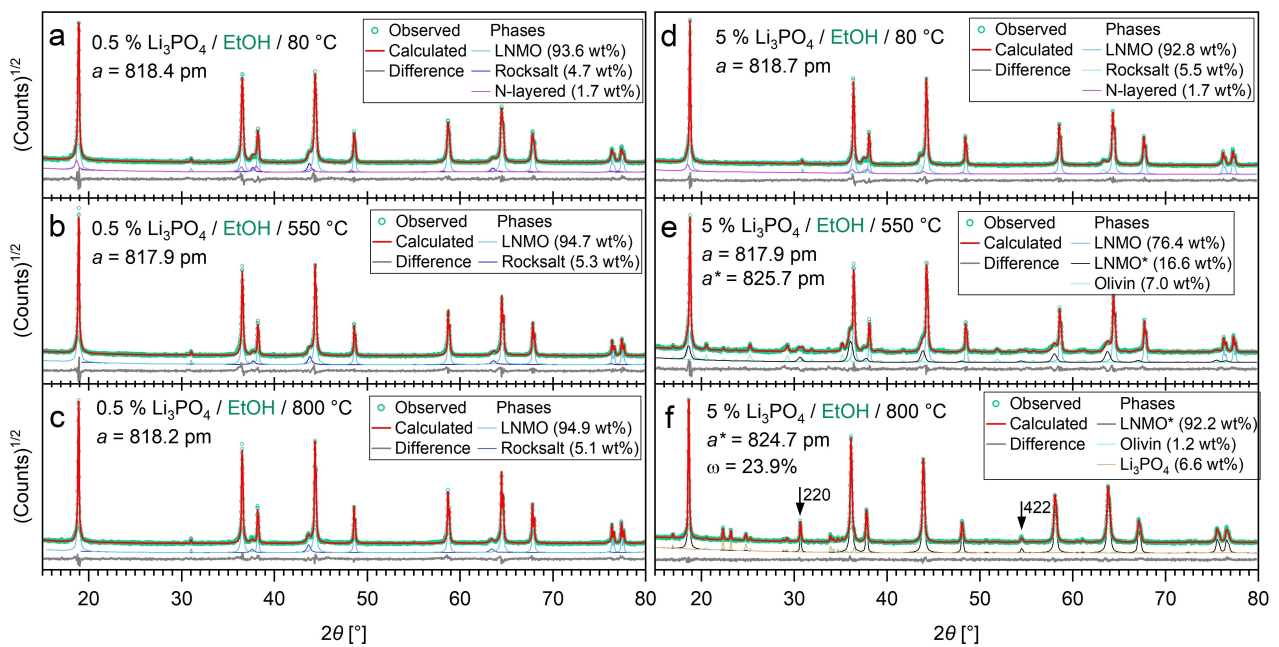


Figure 6. Rietveld refinements of the different LNMO materials coated with the ethanol method with 0.5 and 5.0 wt% Li₃PO₄ after thermal treatments at 80, 550 and 800 °C. The contributions of the individual crystalline phases are shown and set off vertically for the sake of clarity. Increased intensities of the 220 and 422 spinel phase reflections are marked by black arrows and indicate the occupation 23.9% of the Li-site with transition metal ions. The corresponding composition of the LNMO* phase is estimated to be around Li_{0.76}Ni_{0.5}Mn_{1.74}O₄.

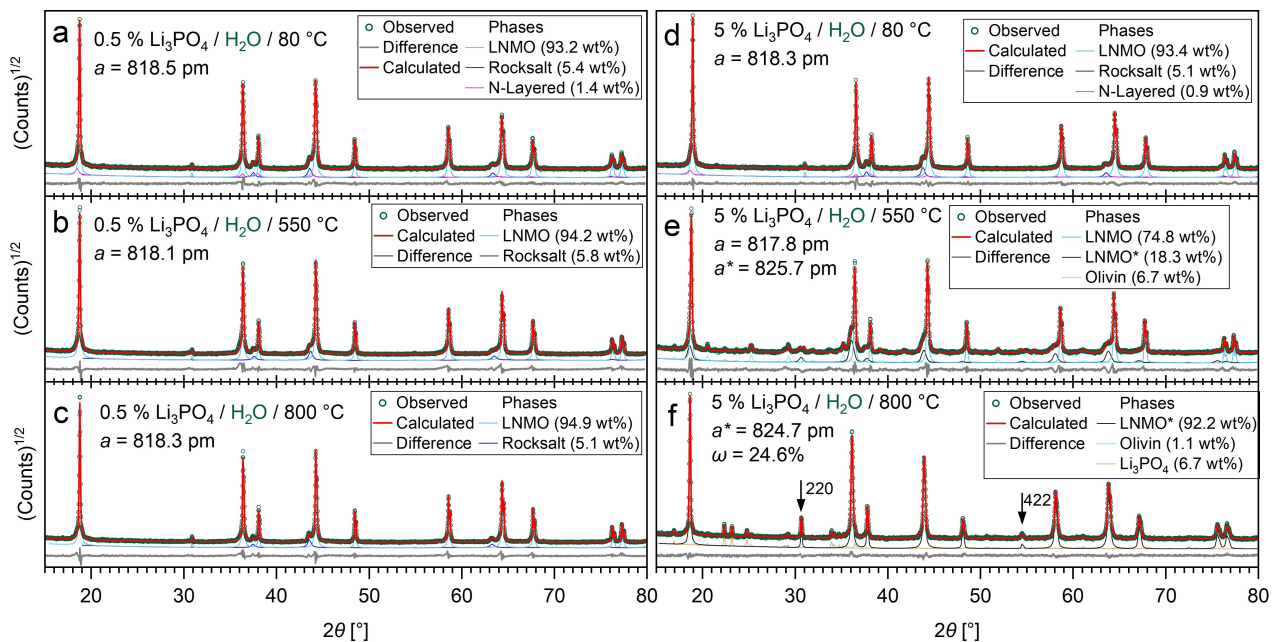


Figure 7. Rietveld refinements of the different LNMO materials coated with the water method with 0.5 and 5.0 wt% LP after thermal treatments at 80, 550 and 800 °C. The contributions of the individual crystalline phases are shown and set off vertically for the sake of clarity. Increased intensities of the 220 and 422 spinel phase reflections are marked by black arrows and indicate the occupation 24.6% of the Li-site with transition metal ions. The corresponding composition of the LNMO* phase is estimated to be around Li_{0.75}Ni_{0.5}Mn_{1.75}O₄.

in the samples coated with 0.5 and 5.0 wt% LP dried at 80 °C (cf. Figures 5-7a and d). The corresponding phase fractions for the N-layered phase were reduced to 0.9–1.7 wt% (see Table 1). The LNMO phase fractions and lattice parameters of the samples dried at 80 °C are similar to those of the pristine sample. The reduced proportion of the N-layered phase

indicates that this Li and Ni-rich side-phase is partially decomposed during the coating process in water and ethanol. Apart from that, no pronounced solid-state reactions take place during the coating processes and drying at 80 °C. One deviation from this is observed in the sample coated using the H₂O method and 5 wt% LP. As shown in Figure 5d, the N-layered

secondary phase can no longer be observed. Instead, numerous new reflections prove the formation of a new crystalline side phase. Despite thorough literature research and comparison with common databases (PDF, ICSD, and COD), it was not possible to assign a phase here. A detailed illustration including all unidentified reflections can be found in the SI, Figure S1.

Besides the presence of the $\text{LiNi}_{0.5-x}\text{Mn}_{1.5+x}\text{O}_4$ spinel main phase, the diffraction patterns of all samples coated with 0.5 wt% LP and calcined at 550 and 800 °C showed the typical reflections of a rock-salt secondary phase (cf. subfigures b and c in Figures 5–7). For the vast majority of samples, the lattice parameter of LNMO is refined to rather common values of 817.9–818.5 pm and the proportion of the minor phases ranges from ~5.1 to 5.8 wt%, which is similar to pristine LNMO and very common for typical disordered LNMO materials.^[1] Voltage profiles shown in Figure S7 confirm similar LNMO phase compositions with almost the same Mn^{3+} content. These similarities strongly indicate that the spinel phase remains vastly unchanged when 0.5 wt% LP are applied as a coating agent. Only the sample coated with 0.5 wt% LP using the H_2O_2 method shows a remarkable increase in the lattice parameter of the LNMO phase to 818.8 pm. Given that this sample's capacity is slightly reduced compared to the corresponding samples coated using H_2O and EtOH (vide infra), it can be assumed that some Li may be lost during the coating process and that Ni or Mn may occupy to a small extent the Wyckoff position 8b of the spinel phase, which is known to increase the spinel phase's lattice parameter.^[1]

In accordance with the observation that the capacity of this sample is slightly diminished in comparison to the corresponding samples coated using H_2O and EtOH (see infra), it can be inferred that some Li may have been lost during the coating process, and that the Wyckoff position 8b of the spinel phase may be partially occupied by Ni or Mn, which is known to result in an increase in the lattice parameter of the spinel phase. However, regarding the detailed values listed in Table 1, it should be emphasized that the estimated standard deviations (e.s.d.) resulting from the Rietveld method systematically underestimate the actual measurement errors. To obtain realistic probable measurement errors, the e.s.d. values have to be multiplied by a factor of about 3.^[36] Furthermore, given the uncertainty regarding the precise composition of the secondary phases and the strong overlap of the LNMO reflections, the errors of the phase fractions still exceed these values, and the probable errors of the phase fractions may be as high as 0.5 percent. Unlike in optimized diffractometers,^[23,37] we estimate that for the lattice parameters refined here, deviations up to 0.3 pm may be attributed to deviations in sample preparation and the Bragg-Brentano geometry, and therefore should not be overinterpreted.

Crystalline phases originating from the coating process cannot be detected in either of the diffraction patterns of the samples coated with 0.5 wt% LP. This, however, is not surprising for two reasons. First, the reflection intensity of phases with 0.5 wt% may not suffice to stand out from the general noise of the data points of the diffraction patterns. Secondly, due to the very thin coating layers, which are

expected to be <6 nm in average (vide supra), reflections would be extensively widened due to crystal size broadening.

To overcome this problem, the 5 wt% LP-modified samples were used to analyze crystalline coating products by means of PXRD and to get insights on interactions with the LNMO main phase and secondary phases. The diffraction patterns and refinements are shown in Figures 5–7d–f at the right-hand side.

The samples coated with 5 wt% LP and only dried at 80 °C using the EtOH and H_2O methods are shown in Figures 6d and 7d. The lattice parameters of the LNMO phase were refined to 818.3 and 818.7 pm and thus are comparable to the pristine sample. Likewise, essentially the same phase composition as in the pristine material can be found, indicating that no extensive reactions with the LNMO phase occur. As already mentioned above, different behaviour is observed in the sample coated using the H_2O_2 method, where a new crystalline phase is formed after drying at 80 °C (Figure 5d).

For the samples coated with 5 wt% LP and calcined at 550 and 800 °C, the diffraction patterns deviate significantly from pristine LNMO, as shown in Figures 5–7e and f. At 550 °C the presence of an olivin-type phase is uniformly observed, which could be refined very well as LiMnPO_4 (s.g. Pnma , $a = 1044.5$ pm, $b = 610.2$ pm, $c = 474.3$ pm), structure model from Ref.,^[38] yielding phase fractions of 6.7–8.3 wt%. The refined olivin-phase lattice parameters listed in Table 1 are fully consistent with those mentioned for LiMnPO_4 , which is a strong indication that a pure LiMnPO_4 -phase or a Mn-rich olivine phase ($\text{Li}(\text{Ni}/\text{Mn})\text{PO}_4$) is formed. In contrast, the presence of LiNiPO_4 or Ni-rich mixed phases can be ruled out due to the mismatch of lattice parameters. To prove this conclusion, the EDS together with SEM analysis was performed in order to get a semi-quantitative idea of the constituents of the studied materials (Figure S6). From the EDS/SEM analysis of 5 wt% LP, 550/800 °C samples, no particles were found that contained more nickel than manganese; the opposite was the case: as shown by the EDS results, the analyzed crystalline blocks (Figure S6) exhibit increased manganese and phosphorus contents, which supports the conclusion from XRD that the presence of LiNiPO_4 or Ni-rich mixed phases can be excluded. Since the coating solution does not contain any extra Mn or Ni ion sources, the formation of LiMnPO_4 has to be due to Mn/Ni extraction from the pristine material. On closer consideration, taking into account high concentrations of phosphate anions and aggressive reaction conditions, such an extraction is not surprising and may happen either during the coating reaction or during the calcination at 550 and 800 °C.

The Rocksalt secondary phase is no longer detectable in these samples and the broad shoulders of the reflections of the LNMO phase clearly indicate a solid state of the coating material on the surface of the spinel phase. At 550 °C reflections indicating crystalline LP are not observed and it is considered, that even if LP exists at this temperature, then only in amorphous state. However, the existence of such amorphous LP is unlikely from a mathematical standpoint. The phosphate ions present in the sample are quantitatively bound in the olivine phase if the equivalent of 5 wt% of LP is added during

the coating process, as only 6.8 wt% LiMnPO₄ should be capable of forming.

The reflections for crystalline LP are finally observed for all 5 wt% LP coated samples calcined at 800 °C (cf. Figure 5–7f). Here, refinements with a structure model of γ -Li₃PO₄^[39] (*Pcmn*, *a*=492.6 pm, *b*=612.9 pm, *c*=1048.3 pm) yielded phase fractions of 5.1–6.7 wt%. It also becomes obvious the proportion of the olivine phase is decreased noticeably to 1.1–2.6 wt%, which clearly indicates that Li₃PO₄ forms from the olivine phase.

Just like for the samples calcined at 550 °C, the reflections of the Rocksalt secondary phase ($2\theta=\sim 38^\circ$ and $\sim 44^\circ$) can no longer be observed. It is anticipated that the impurity phases will react with the phosphates resulting in LiMPO₄ on the surface of the LNMO material. A further remarkable feature in the samples coated with 5 wt% LP is the change of intensities and positions of the reflections of the spinel phase. At 800 °C, the reflections are shifted towards lower angles, and the refinements consistently yield significantly enlarged lattice parameters of 824.4 pm to 824.7 pm, which are beyond the range of typical LNMO cathode active materials. Furthermore, the increase of the intensity of the 002 and 422 reflections are a clear indication for a partial occupation of the Wyckoff site 8b site with transition metal ions. As applied earlier,^[1] during the refinement process, a structure model with a site mixing parameter ω was used, allowing for the partial substitution of Li by Mn on Wyckoff site 8b according to Li_{1- ω} Mn _{ω} Ni_{0.5}Mn_{1.5}O₄. Here, ω values of 0.239(2) to 0.265(2) were refined, which corresponds to spinel phase compositions of Li_{0.76}Ni_{0.5}Mn_{1.74}O₄ to Li_{0.73}Ni_{0.5}Mn_{1.77}O₄. This finally yields a conclusive explanation for the increased lattice parameter of the spinel phases, which correspondingly are labelled as LNMO* in Figures 5–7. The occupation of the tetrahedral position of the spinel phase by transition metal ions during calcination is by no means unusual.^[1] Normally, however, these processes are largely reversible, so that typical LNMO compositions are recovered during cooling of the samples. In the present case, however, the reversibility of this process appears to be prevented by the coating, presumably due to the preferential crystallization of γ -Li₃PO₄.

In the 550 °C samples (cf. Figures 5–7e) the spinel phase shows a similar behaviour, however, the main phase reflections are not completely shifted, but there are broad shoulders towards low diffraction angles. This indicates that a similar reaction occurs at 550 °C, but mainly on the surface. In order to roughly approximate the mass fraction of LNMO participating in the reaction process, beside LNMO the LNMO* phase (*a*≈825 pm) was introduced to these Rietveld refinements, and yielded phase fractions of about 17–28 wt%. The core of the LNMO particles most likely remains unaffected, as the main LNMO phase still yields almost the same lattice parameter as the pristine material.

Overall, it can be concluded that the coating method in water, ethanol and hydrogen peroxide essentially involves the same processes and yield the same products after calcination. Only the phase proportions vary slightly. The 5 wt% LP coated samples show that the reaction paths are complex and LNMO, secondary phases and coating material influence each other.

Although the target compound – crystalline Li₃PO₄ – is obtained after calcination at 800 °C, it is obvious that a Mn-rich olivine phase Li(Mn/Ni)PO₄ is formed as an interstitial after the calcination at 550 °C and the spinel phase is depleted of Li during the calcination process. Most likely, such negative side-effects are negligible at low target concentrations like 0.5 wt% LP. Nonetheless, consistent with previous studies,^[14,16,17] it is evident once more that coatings on the spinel surface that do not involve extensive solid state reactions are arduous to attain and are likely only feasible at low calcination temperatures (< 600 °C).

Electrochemistry

It is important to note that the pristine active material used in this work shows comparatively low capacity fading and good capacity retention. The spinel particles, normally, exhibit mainly {111} surfaces. The powder used in this work contains a large number of particles with truncated {100} surfaces, which seems to promote lithium ions transport.^[40] However, compared to many commercially available spinel products, the one used in this work does not show the lowest long-term capacity fading or the best capacity retention. The goal of this study, however, was not to make the perfect spinel material, but to test how well an uncoated sample works and a coated one that was treated the same way. This would help us figure out what the coating does.

The reason for the somewhat reduced capacity of the pristine sample compared to the samples calcined at 800 °C can be explained by the phase composition. The pristine sample contains a Li-rich side phase (N-layered). Therefore, the pristine LNMO phase is slightly deficient in Li, since the Li-site is occupied by TM ions. This reduces the capacity of the pristine sample. Figures 8 and 9 show how LP-modified LNMO samples perform electrochemically. Several samples were chosen: the pristine, the references (pristine heated at 550 and 800 °C) and coated samples, with 0.5 wt% LP, heated at 550 and 800 °C. The samples coated with 5.0 wt% LP were not examined electrochemically for obvious reasons, e.g. because of too thick coating layer and presence of additional products that may not be part of the coating. To assess the electrochemical performance of uncoated and coated LNMO materials coin-type half-cells at voltage window of 3.5–4.9 V have been used.

The differential capacity versus potential (dQ/dV versus V) data are presented in Figure S8. From the tenth cycle onwards, no significant alteration in the dQ/dV versus V behaviour is observed. In the voltage region of 4.7–4.8 V two pairs of redox peaks related to the Ni²⁺/Ni³⁺ and Ni³⁺/Ni⁴⁺ couples are observed. A broad and weak peak associated with the Mn³⁺/Mn⁴⁺ couple is also observed at about 4.0 V (not shown). A deeper look onto dQ/dV versus V results for the samples treated at 800 °C shows some differences between the materials. For the uncoated LNMO and calcined at 800 °C, the two high voltage peaks constantly shift to higher voltages on cycling, suggesting an increase in polarization and impedance. For the coated materials, LNMO-LP-800H, LNMO-LP-800E and LNMO-LP-

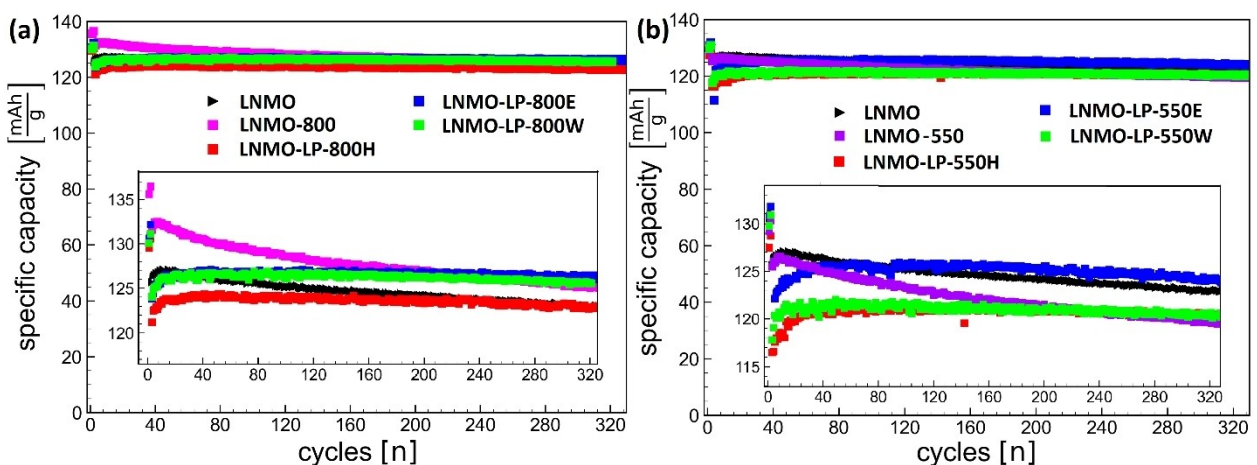


Figure 8. Capacity retention test at charge-discharge rate at C/20 -C (one (first) cycle at 0.05 C, two cycles at 0.1 C, and then charged (at 0.5 C) and discharged (at 1 C) for uncoated and coated and calcined at 800 °C (a) and at 550 °C (b). Inset: zoomed version of the graphs.

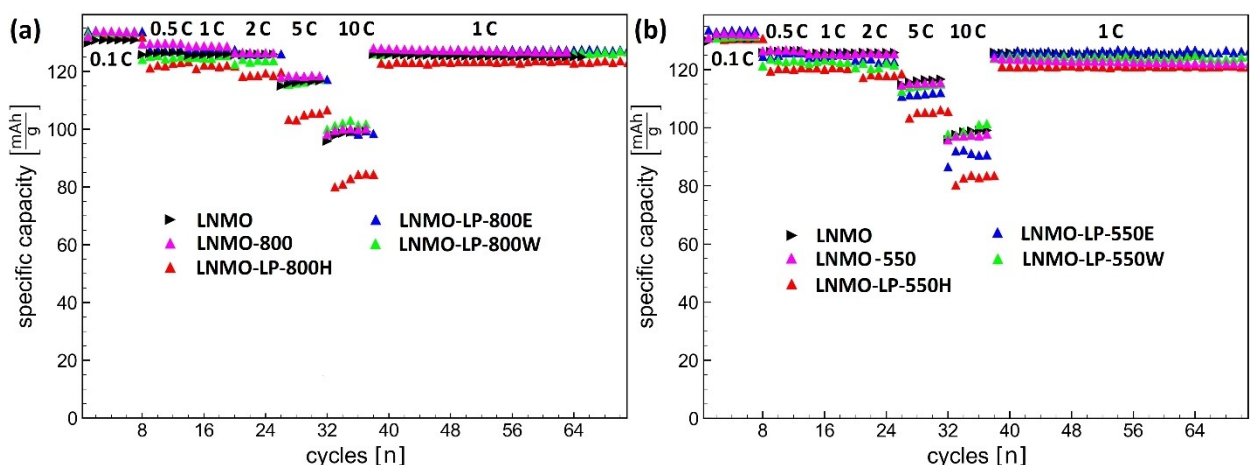


Figure 9. Rate capability test (the first cycle was done at 0.05 C; charge rate was C/2 without holding the voltage and discharge rates were varied as indicated in the figure) of ten samples: bare (LNMO), bare calcined at 800 °C (a)/550 °C (b), coated with different methods and calcined at 800 °C (a)/550 °C (b).

800W, however, the increase in polarization is less pronounced, suggesting a stabilization of the interfaces due to the coating. A similar effect was previously reported for a LP coated LNMO doped with titan and aluminum^[16] and a Fe–Ti doped LNMO material with an LP additive.^[10]

The capacity retention of present materials, for mass loading of 3–4 mg/cm² and in the 3.5–4.9 V cycling regime, of bare LNMO and LNMO calcined at 550 and 800 °C, coated and calcined at 550 and 800 °C, is shown in Figure 8. A test cell for one of the materials was made, cycled in the 3.5–5.0 V regime and the result was the same as for the cell cycled between 3.5 and 4.9 V.

The cells were initially charged-discharged one cycle at 0.05 C, two cycles at 0.1 C, and then charged (at 0.5 C) and discharged (at 1 C) more than 300 times. It should be mentioned, that the discharge capacities of the initial several (~10–20) cycles for all samples show a growing trend and then get stabilised. Such effects are not new and it is suggested that during the first cycles the electrodes are being better wetted and activated. Therefore as initial capacities were taken those

after ~10–20 cycles. From the obtained results, it is clear that LP-treated materials are all superior to the untreated LNMO. The bare LNMO and LNMO-800 show initial capacities of ~127 and 133.0 mAhg⁻¹, respectively, however, both electrodes show a comparable degree of capacity fading: after 320 cycles the remained capacity for the original LNMO is ~96.9% and for the LNMO-800 – ~94.6%. On the other hand, LNMO-LP-800H, LNMO-LP-800E and LNMO-LP-800W (initial capacities ~123.5, 126.0 and 126.0 mAhg⁻¹, respectively) show a much higher stability and capacity retention: for the LNMO-LP-800H the remained capacity is ~99.4% and for LNMO-LP-800E and LNMO-LP-800W – almost 100%. In addition to negligible difference in the remained capacity, LNMO-LP-800H also has a ~2% smaller capacity in comparison to other two cells. This may be due to more aggressive reaction conditions for LNMO-LP-800H, which resulted to slight decomposition of the LNMO surface.

To determine the influence of the morphology and crystallinity of the coating layer on the electrochemical properties, as mentioned above, the coated samples were calcined at two purposefully chosen temperatures: 550 and 800 °C. In

addition, the pristine LNMO was also heated at the same temperatures. This was done because the thermal treatment can have an impact on the phase composition and secondary phase ratio, and, respectively, electrochemical performance.^[1] It is important to note that this is a necessary step, which must always be followed when comparing the electrochemistry of an uncoated material with the electrochemistry of a coated one. This step is ignored in almost all studies made in this field. Although we are currently unable to verify this with alternative methods, it can be inferred that the coating layers of samples coated with 0.5 wt% LP exhibit identical composition as those of samples coated with 5 wt% LP, albeit with a distinct thickness. In addition, LP at these two temperatures has different crystallinity and at 550°C it is most probably in form of LiMnPO₄ (vide supra). Remarkably, the LNMO-LP-550E and LNMO-LP-800E cathode materials synthesised in ethanol show a very similar initial capacity, ~125 and ~126 mAhg⁻¹, respectively, and a comparable degree of capacity fading. The most feasible reason for this effect is that in this specific case (reaction in Ethanol) the coating retains its protecting properties and the temperature seems to not influence the structure and electrochemical properties of the active material.

The rapidity of the Li-ion extraction and insertion from and into the cathode active material is very important when the charging time of a battery is supposed to be amended. Such a test was performed in the same range of 3.5–4.9 V and at different rates from 0.1–10 C (Figure 9). The cells were first charged-discharged at a current density of 0.05 C for one cycle and six cycles at 0.1 C. Then they were charged with 0.5 C rate and discharged at 0.5, 1, 2, 5 and 10 C rates, respectively. After 10 C, the cells were further cycled at 1 C. All cells but those assembled from materials coated in H₂O₂ show very similar behaviour and are in agreement with the results obtained from the capacity retention tests. At high rates as 5 and 10 C the cells obtained from the materials coated in H₂O₂ show a slightly lower capacity in comparison to other cells. The reason could most likely be more aggressive synthesis conditions that, to some extent, changed the structure of the active material and this affects the electrochemical processes at high discharging rates. Remarkably, once the electrode was cycled at 10 C and the current density proceeds back to 1 C, the initial capacity observed earlier at 1 C for LNMO-LP-800H and LNMO-LP-550H samples is recuperated and further cyclisation is very stable. Although at 0.5, 1, 2, 5 and 10 C rates all cells show very similar capacity retention and the same minor degree of capacity fading, once the discharge rate decreases from 10 C back to 1 C, the cells with uncoated materials show a much higher degree of capacity fading. Hence, the capacity retention and rate capability of the LNMO cathodes was not improved by the additional heating, but by the coating, with the higher capacity retention and better performance obtained for the samples coated in ethanol and water, and calcined at 800°C.

Additional conclusions regarding the positive contribution of the coating were drawn from differential capacity versus potential curves of the uncoated and coated samples, which were calcined at 800°C. From the capacity retention tests, in Figure S8, the dQ/dV curves for the nickel redox couples are

extracted for the range between 100th and 300th cycles. The analysis of these curves points to another remarkable observation, which points to the positive input of the coating in water in comparison to ethanol or H₂O₂. All the peaks for LP-modified spinel coated in H₂O₂, ethanol, or water are the same shape, but the polarization of the coated material in water is smaller than that of the coated material in ethanol or H₂O₂.

Although the specific energy of the spinels coated in ethanol and water is the same (~575 mWh/g), the energy (99.6%) and coulombic efficiency (~100%) (Figure S9) of the sample coated in water are higher than for the sample coated in ethanol. Furthermore, Figure S9 indicates that the specific internal resistance of the "water" sample (~60 Ωcm²) is smaller and more constant throughout the analyzed cycle interval compared to the "ethanol" sample (~80 Ωcm²), which may indicate a faster ionic migration through the coating layer in the "water" sample. All these results suggest a good cycling performance for LNMO-LP800E and a better one for LNMO-LP800W. To find out why water works better for coating LNMO with LP, more experiments and advanced methods are needed. These will be studied in the future.

Conclusions

In summary, it was possible to synthesize LP-coated LiNi_{0.5}Mn_{1.5}O₄ material using hydrogen peroxide as an activating reagent. These reactions can be carried out in both concentrated hydrogen peroxide solutions and organic or aqueous diluted solutions. Samples coated with 5 wt% LP indicate that the coating reactions in ethanol, water and hydrogen peroxide are very similar and yield the same calcination products. The calcination at 550°C leads to a quantitative formation of an Olivin-type surface layer with the composition Li(Mn/Ni)PO₄. After calcination at 800°C, the Olivine-type phase is further transformed into crystalline LP. For the samples coated with 0.5 wt% LP, a coating layer thickness of 6 nm is expected on the LNMO surface. XRD investigations have confirmed that the utilization of coating reagents at such low concentrations has negligible effects on the composition of the LNMO spinel phase. The samples coated with 0.5 wt% show decent cycling behavior indicating that the coating layer can suppress the decomposition of the active material, by protecting it from direct communication with electrolyte.

The electrochemical results of nine samples and their comparison lead to the conclusion that, in general, the protective effects of the coating layer are almost identical, with a few exceptions, and there is no significant difference between them. All three approaches are possible to use in the lab and in industry. It will depend on the tasks and requirements of the production group, such as getting the coated product fast and working under risky and strictly controlled conditions, or getting it slowly and safely.

For all three approaches one can use different other lithium compounds, e.g. LiOH, Li₂CO₃ or Li₂O. It should be, however, noted that the success of such reactions will depend on the

solubility of the coating components (all components must be soluble) in the solvents used for the coating reaction.

The approach presented in this work can be easily extended to different other cathode active materials, e.g. layered oxides. The preliminary tests show that even nickel-rich (90–93%) layered oxides are possible to protect with LP in alcoholic solutions using this method, thus opening a new way for the designing of fast and low-cost coating approaches. The application of this method to sodium-containing active cathode materials is also in progress.

Acknowledgements

This work was carried out with the support of the Helmholtz Energy Materials Foundry (HEMF), a large-scale distributed research infrastructure founded by the German Helmholtz Association. It also contributes to the research performed at CELEST (Center for Electrochemical Energy Storage Ulm-Karlsruhe). Dr. Thomas Bergfeldt (Karlsruhe Nano Micro Facility, KNMF, www.knmf.kit.edu), is acknowledged for the support with elemental analysis. The authors gratefully acknowledge the funding from Bundesministerium für Bildung und Forschung (BMBF) within the FESTBATT, Cluster of Competence for Solid State Batteries (grant number 03XP0433A). We also thank Margarete Offermann for support on surface area analysis. Open Access funding enabled and organized by Projekt DEAL.

Conflict of Interests

The authors declare no conflict of interest.

Data Availability Statement

The data that support the findings of this study are available from the corresponding author upon reasonable request.

Keywords: Li₃PO₄ (LP) · X-ray diffraction · LiNi_{0.5}Mn_{1.5}O₄ Lithium ion batteries · Cathode materials · Electrochemical properties · Particle coating

- [1] P. Stüble, V. Mereacre, H. Gesswein, J. R. Binder, *Adv. Energy Mater.* **2023**, *13*, 2203778.
- [2] I. Belharouak, W. Lu, D. Vissers, K. Amine, *Electrochem. Commun.* **2006**, *8*, 329–335.
- [3] J. R. Dahn, E. Fuller, M. Obrovac, U. Vonsacken, *Solid State Ion.* **1994**, *69*, 265–270.
- [4] Y. Kobayashi, H. Miyashiro, K. Takei, H. Shigemura, M. Tabuchi, H. Kageyama, T. Iwahori, *J. Electrochem. Soc.* **2003**, *150*, 1577–1582.
- [5] Y. Wu, L. Ben, H. Yu, W. Qi, Y. Zhan, W. Zhao, X. Huang, *ACS Appl. Mater. Interfaces* **2019**, *11*, 6937–6947.
- [6] S. Yubuchi, Y. Ito, T. Matsuyama, A. Hayashi, M. Tatsumisago, *Solid State Ion.* **2016**, *285*, 79–82.
- [7] H. Luo, H. Chen, X. Luo, Z. Liu, H. Zhou, *J. Mater. Sci: Mater. Electron.* **2022**, *33*, 6872–6887.

- [8] N. R. Park, Y. Li, W. Yao, M. Zhang, B. Han, C. Mejia, B. Sayahpour, R. Shimizu, B. Bhamwala, B. Dang, S. Kumakura, W. Li, Y. S. Meng, *Adv. Funct. Mater.* **2024**, *34*, 2312091.
- [9] M. Hofmann, F. Nagler, M. Kapuschinski, U. Guntow, G. A. Giffin, *ChemSusChem* **2020**, *13*, 5962–5971.
- [10] P. Stüble, M. Mueller, T. Bergfeldt, J. R. Binder, A. Hofmann, *Adv. Sci.* **2023**, *10*, 2301874.
- [11] J. He, G. Melinte, M. S. Dewi Darma, W. Hua, C. Das, A. Schökel, M. Etter, A.-L. Hansen, L. Mereacre, U. Geckle, T. Bergfeldt, Z. Sun, M. Knapp, H. Ehrenberg, J. Maibach, *Adv. Funct. Mater.* **2022**, *32*, 2207937.
- [12] J. Chong, S. Xun, X. Song, G. Liu, V. S. Battaglia, *Nano Energy* **2013**, *2*, 283–293.
- [13] J. Chong, S. Xun, J. Zhang, X. Song, H. Xie, V. S. Battaglia, R. Wang, *Chem. Eur. J.* **2014**, *20*, 7479–7485.
- [14] V. Mereacre, P. Stüble, A. Ghamlouche, J. R. Binder, *Nanomaterials (Basel)* **2021**, *11*, 548–560.
- [15] V. Mereacre, N. Bohn, M. Müller, S. Indris, J. R. Binder, *Mater. Res. Bull.* **2021**, *134*, 111095.
- [16] V. Mereacre, N. Bohn, P. Stüble, L. Pfaffmann, J. R. Binder, *ACS Appl. Energy Mater.* **2021**, *4*, 4271–4276.
- [17] V. Mereacre, P. Stüble, V. Trouillet, S. Ahmed, K. Volz, J. R. Binder, *Adv. Mater. Interfaces* **2022**, *10*, 2201324.
- [18] M.-H. Chiou, K. Borzutzki, J. H. Thienenkamp, M. Mohrhardt, K.-L. Liu, V. Mereacre, J. R. Binder, H. Ehrenberg, M. Winter, G. Brunklaus, *J. Power Sources* **2022**, *538*, 231528.
- [19] M. A. Hasan, M. I. Zaki, L. Pasupulety, K. Kumari, *Appl. Catal. A: Gen.* **1999**, *181*, 171–179.
- [20] S. B. Kanugo, K. M. Parida, B. R. Sant, *Electrochim. Acta* **1981**, *26*, 1157–1167.
- [21] J. N. Park, J. K. Shon, M. Jin, S. H. Hwang, G. O. Park, J. H. Boo, T. H. Han, J. M. Kim, *Chem. Lett.* **2010**, *39*, 493495.
- [22] H. M. Rietveld, *J. Appl. Cryst.* **1969**, *2*, 65–71.
- [23] H. Geßwein, P. Stüble, D. Weber, J. R. Binder, R. Möning, *J. Appl. Cryst.* **2022**, *55*, 503–514.
- [24] C. Bohnke, B. Rerag, F. Le Berre, J.-L. Fourquet, N. Randriantoandro, *Solid State Ion.* **2005**, *176*, 73–80.
- [25] S. Koblyanskaya, O. Gavrilenko, A. Belous, *Russ. J. Inorg. Chem.* **2013**, *58*, 637–647.
- [26] I. C. Popovici, E. Chirila, V. Popescu, V. Ciupina, G. Prodan, *J. Mater. Sci.* **2007**, *42*, 3373–3377.
- [27] Y.-R. Zhu, J. Yuan, M. Zhu, G. Hao, T.-F. Yi, Y. Xie, *J. Alloys Compd.* **2015**, *646*, 612–619.
- [28] H. Zhang, T. Yang, Y. Han, D. Song, X. Shi, L. Zhang, L. Bie, *J. Power Sources* **2017**, *364*, 272–279.
- [29] C.-H. Jo, D.-H. Cho, H.-J. Noh, H. Yashiro, Y.-K. Sun, S. T. Myung, *Nano Res.* **2015**, *8*, 1464–1479.
- [30] H. G. Song, J. Y. Kim, K. T. Kim, Y. J. Park, *J. Power Sources* **2011**, *196*, 6847–6855.
- [31] F. Wu, X. X. Zhang, T. L. Zhao, L. Li, M. Xie, R. J. Chen, *J. Mater. Chem. A* **2015**, *3*, 9528–9537.
- [32] X. F. Bian, Q. Fu, X. F. Bie, P. L. Yang, H. L. Qiu, Q. Pang, G. Chen, F. Du, Y. J. Wei, *Electrochim. Acta* **2015**, *174*, 875–884.
- [33] X. W. Li, R. Yang, B. Cheng, Q. Hao, H. Y. Xu, J. Yang, Y. T. Qian, *Mater. Lett.* **2012**, *66*, 168–171.
- [34] Y. Lee, J. Lee, K. Y. Lee, J. Mun, J. K. Lee, W. Choi, *J. Power Sources* **2016**, *315*, 284–293.
- [35] W. Li, J. N. Reimers, J. R. Dahn, *Phys. Rev. B* **1992**, *46*, 3236–3246.
- [36] J.-F. Bérar, P. Lelann, *J. Appl. Cryst.* **1991**, *24*, 1–5.
- [37] P. Stüble, J. R. Binder, H. Geßwein, *Electrochim. Sci. Adv.* **2022**, *2*, e2100143.
- [38] N. V. Urusova, M. A. Semkin, S. Lee, Yu. A. Barykina, D. G. Kellerman, A. E. Teplykh, N. Pirogov, A. S. Volegov, Yu. N. Skryabin, *Ferroelectrics* **2017**, *509*, 74–79.
- [39] O. S. Bondareva, M. A. Simonov, N. V. Belov, *Dokl. Akad. Nauk SSSR* **1978**, *240*, 75–77.
- [40] H. Liu, R. Kloepsch, J. Wang, M. Winter, J. Li, *J. Power Sources* **2015**, *300*, 430–437.

Manuscript received: October 15, 2024
Revised manuscript received: November 22, 2024
Version of record online: December 4, 2024